# LINE BONDING OF WAFERS USING TRANSMISSION LASER BONDING TECHNIQUE FOR MICROSYSTEM PACKAGING

Jong-Seung Park and Ampere A. Tseng
Department of Mechanical and Aerospace Engineering
Arizona State University
Tempe, Arizona, USA, 85287
Phone: (480) 965-8201
Fax: (480) 965-1384
Email: ampere.tseng@asu.edu

## ABSTRACT

The transmission laser bonding (TLB) technique can not only satisfy wafer level bonding requirements but also be directly implemented into the existing semiconductor production line. Using a nanosecond pulsed Nd:YAG laser, Pyrex glass-to-silicon wafers were successfully bonded by uniformly spaced individually bonded spots. The bond strength resulting from use of the TLB technique is comparable to the strength of the bond produced by bonding techniques currently used in microsystem or micro-electro-mechanical system (MEMS) packaging. In addition to packaging, the TLB technique can also be used to conveniently assemble and encapsulate miniature devices with selective bonding areas. In this paper, the continuous line bonding produced by the TLB technique has been implemented and characterized using various sets of bonding conditions. In this paper, TLB is used to make continuous line bonding of Pyrex and silicon wafers. Continuous line bonds are typically generated by overlapping single bond spots, in which the overlapping is achieved by varying the laser scanning speed as it pastel across the wafers. This results in a wide range of laser energy density (absorbed laser fluence). The specific effects of laser energy are examined and evaluated in order to define the laser operation window which provides the optimal conditions for reliable line bonding. In addition to the bond strength evaluation, the bonded interface is analyzed by Auger Electron Spectroscopy (AES) and X-ray Photoelectron Spectroscopy (XPS) to quantify the drifting or diffusion of atoms that occurs between glass and silicon wafers during the bonding process.

**KEY WORDS**: Wafer bonding, Laser, Silicon, Pyrex, MEMS Packaging

## INTRODUCTION

In micro devices and system fabrication, wafer level bonding offers a unique opportunity to combine different materials, such as a cover substrate being bonded onto a micromachined substrate. Some of the more prominent applications of this technology are Silicon-On-Insulator (SOI) wafers [1], MEMS sensors and actuators [2], and biomedical devices [3]. Conventional wafer bonding techniques, such as anodic bonding, direct wafer bonding, and eutectic bonding, require a high processing temperature and a flat surface. Furthermore, these conventional methods provide little sensitivity in the local selectivity of bonding [4]. The transmission laser bonding (TLB) technique can be conveniently used to bond wafers in ambient conditions. It allows the bonding area to be selectively controlled. Additionally, the TLB process does not require high processing temperatures, high electric potentials, or an intermediate layer, as mandated by conventional wafer bonding processes. For example, fusion bonding requires a high annealing temperature (800-1100 °C) for the creation of voidless high strength bonds, while anodic bonding is best conducted at conditions of high bias voltages (400-1500 V) and relatively high temperatures (200-500 °C) [3].

In the TLB process, the incident laser is transmitted through the transparent cover substrate onto the opaque substrate. The transmitted laser energy is concentrated near the surface of the opaque substrate. This highly focused, high-density energy source melts a small portion of the opaque substrate (Fig. 1), resulting in a fusion joint forming between the two substrates. The thermal coefficient of the transparent substrate should be identical to that of the opaque substrate in order to avoid the coating of strain and thermal stress in the joints [3].

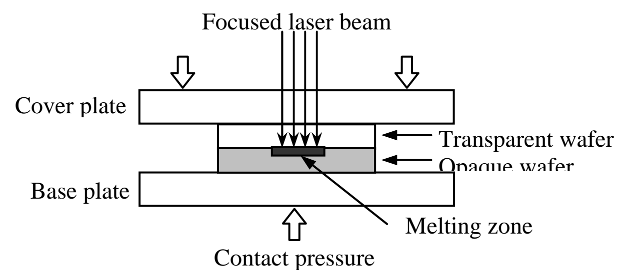


Fig. 1 Schematic of laser bonding

Using a continuously emitting Nd:YAG laser with a 1064 nm wavelength, Wild et al. [4] and Witte et al. [5] demonstrated the reproducible bonding of silicon-glass wafers with a 300-μm focused beam diameter. Wild et al. used 30 W laser emission powers to generate $4 \times 4$ mm² circle- and square-contour bonds. In dynamic experiments, cracks were generated in the glass at the beginning or end of the bonded line due to the high temperature gradient. Tensile test resulted

in a measurement of bond strengths of 5 ~ 10 MPa. Witte et al. defined a narrow parameter window that permits the formation of a circular bond with a 3 mm diameter at 47-W laser power. This article mentioned that melting the silicon would destroy the single crystal, thereby resulting in a poly crystalline structure that changes the electrical and mechanical properties of the original structure. Park and Tseng [6] demonstrated the process of bonding locally selective pyrex-to-silicon wafers with a layout of uniformly spaced individual bond spots (of about 270 μm diameter), using a nanosecond pulsed Nd:YAG laser of 532 nm (Visible, Green) with 200 mJ of pulse energy. A bond strength, as determined by a tensile test, was achieved of approximately 10 MPa. This which is on par with conventional wafer bonding techniques. Critical contact pressure was determined to be 0.5 MPa for the production of reliable laser bonding quality. Using AES (Auger Electron Spectroscopy) and XPS (X-ray Photoelectron Spectroscopy), it was found that the oxygen diffusion from the glass surface toward the melted silicon surface. This resulted in the formation of covalent Si-O bonds between the two wafers. In this paper, continuous line bonding using the TLB technique is demonstrated using a nanosecond pulsed Nd:YAG laser. Pyrex and silicon wafers are bonded by continuous lines, generated by overlapping individual bond locations.

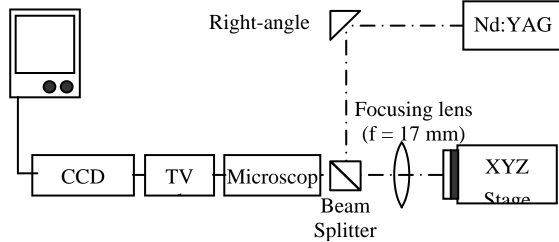


Fig. 2 Schematic of TLB workstation

**LASER FLUENCE IN WAFER BONDING**

In this paper, a nanosecond pulsed Nd:YAG laser is used to the form continuous line bonding. The layout consists of a Nd:YAG laser with its interface controller, refractive and diffractive optics for beam guidance and focusing, and a precision XYZ stage with a sub-micron positioning resolution. The operating wavelength of the Nd: YAG laser is 532 nm (Visible, Green) with 200 mJ of pulse energy. With respect to the 532 nm visible green laser light, the Pyrex wafer is considered to be transparent while silicon wafer is opaque. The laser system provides laser pulses with 7 ns of full width, half maximum (FWHM) pulse duration. The incident laser light is focused by a single lens element (Mitutoyo, M Plan NUV 20) of 17 mm focal length as shown in Fig. 2. The focal plane position is placed at the interface of the two substrates, using the precision XYZ stage and CCD camera. With this setup, a beam diameter approximately 270 μm is obtained at the interface of the two substrates. Single laser pulses (7 ns duration time) are used to obtain one bond spot, successfully achieving localized bonding.

The laser energy density, or fluence distribution, of a focused laser beam can be described by a Gaussian distribution. This distribution can be mathematically represented as:

$$F(r,\sigma) = F_o \exp\left(-\frac{r^2}{\sigma^2}\right)$$

where $F$ is the laser fluence distribution; $F_o$ is the peak fluence at the center; $r$ is the radial coordinate and the beam center is located at $r = 0$; σ is the standard deviation of the Gaussian distribution, in which the beam diameter is 2.828σ where the fluence is $1/e^2$ (13.5%) of its peak fluence ($F_o$). The total incident laser energy ($E_p$) transmitted by the beam can be calculated by integrating the irradiance over the entire cross section, as shown below.

$$E_p = \int_0^{2\pi}\int_0^{\infty} F(r,\sigma) r dr d\theta = 2\pi \int_0^{\infty} F_o \exp\left(-\frac{r^2}{\sigma^2}\right) r dr = F_o \pi\sigma^2$$

In this manner, the peak energy density can be obtained from the total energy ($E_p$) of laser beam. The laser fluence distribution of Gaussian laser beam can be found by:

$$F(r,\sigma) = \frac{E_p}{\pi\sigma^2} \exp\left(-\frac{r^2}{\sigma^2}\right)$$

A continuous line bonding is normally generated by overlapping individual bonded spots. Spot overlapping is achieved by varying the laser scanning speed on the target, resulting in varying laser fluences. A wide range of laser fluences can be achieved by controlling the scanning speed of the laser rather than by needing to vary the input power. For continuous line bonding, the normalized laser fluence distributions (Gaussian beam) over the target substrate, given by x and y coordinates, is represented by

$$\frac{F}{F_o} = \sum_{m=0}^{M} \exp\left(-\frac{(x-np_x)^2}{\sigma^2}\right) \sum_{n=0}^{N} \exp\left(-\frac{(y-np_y)^2}{\sigma^2}\right)$$

where $m$ and $n$ are the number of pulses, $p_x$ and $p_y$ are the pixel spacing determined by the scanning speed ($V$), and the pulse repetition rate ($r_p$), $p_x = V/r_p$. As the laser beam moves along the y direction, the distribution along the y direction represents a summation of the fluence from different laser spots, overlapped by the pixel spacing, $p_x$. The repetition rate for the line is set at a frequency 10 Hz. Therefore, lower speeds cause more overlapping of spots and greater fluence. Fig 3 clearly illustrates the 3D laser fluence distribution profiles for $p_x/\sigma$ equal to 1, 2 and 3. This distribution indicates that a normalized pixel spacing, equal to or smaller than 1, generates a uniform scanning laser fluence. Higher normalized pixel spacing provides a more fluctuating peak fluence.

The normalized peak fluence becomes uniform and converges to a constant of 1.773, and the fluctuation becomes less than 0.01 % when the normalized pixel spacing ($p_x/\sigma$) equals 1. The condition of $p_x/\sigma = 1$ is equivalent to $p_x = 1\sigma = 95.1$ μm. As the normalized pixel spacing increase, the fluence fluctuation increases, as shown in Fig. 4.

**EXPERIMENT**

In the present experiment, 500-μm thick pyrex glass is used as the transmitting substrate while 500-μm thick n-type silicon is used as the absorbing substrate. Since Pyrex glass and silicon have a near equivalent thermal expansion coefficient ($3.25\times10^{-6}$/K), the bonding residue stresses can be minimized.

In order to achieve an intimate contact between two different substrates, clamping pressure in a range of 0.1 ~ 2 MPa is applied to the substrates to be bonded.

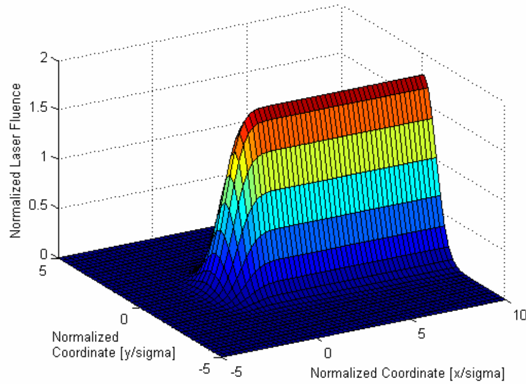


a) Normalized pixel spacing ($p_x$) equals 1

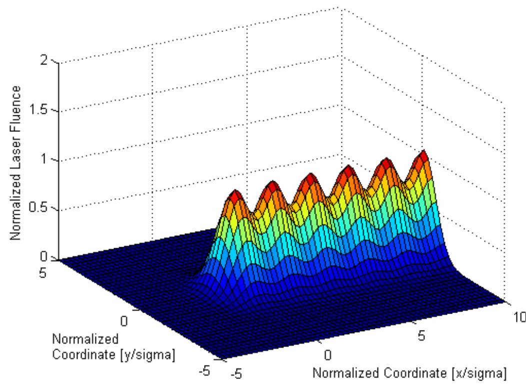


b) Normalized pixel spacing ($p_x$) equals 2

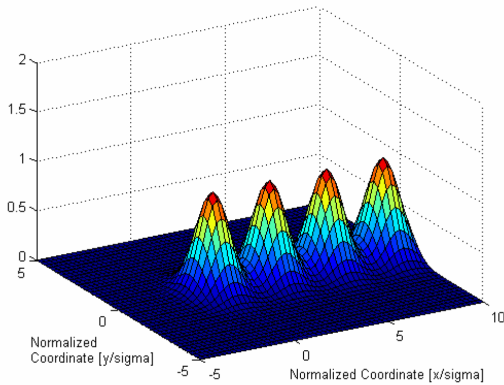


c) Normalized pixel spacing ($p_x$) equals 3

Fig. 3 Simulated normalized laser fluence by different pixel spacing for line bonding

A miniature load cell is responsible for simultaneously measures this during the bonding process. Transparent quartz is used as a cover plate, applying the contact pressure as it allows transmission of the laser beam.

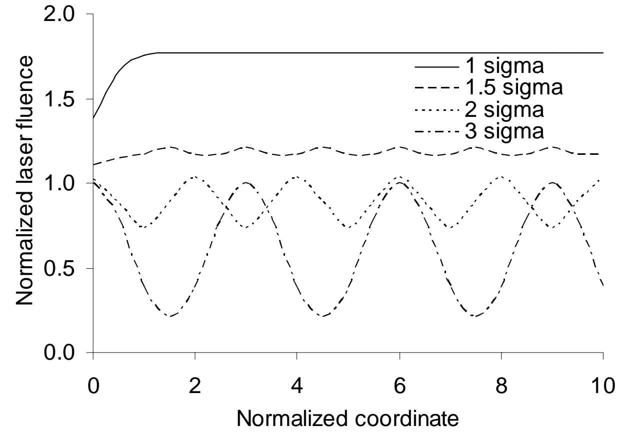


Fig. 4 Laser peak fluence distribution by overlap effect

Repeated laser pulses (7 ns duration time) with a 10-Hz repletion rate are used to obtain a line bond. In order to investigate the line bonding geometry's effect on tensile strength, four pixel spacings ($p_x$) in the x direction are considered: 1σ, 1.5σ, 2σ, and 3σ. The corresponding pixel spacings are 95.1μm, 142.7μm, 190.2μm, and 285.3μm, respectively. The pixel spacing ($p_y$) in y direction is fixed at 1016 μm (11σ). Four different contact pressures are applied for each pixel spacing; 0.1 MPa, 0.5 MPa, 1 MPa and 2 MPa. For a line bonding test, Pyrex and silicon wafers are bonded in 5-mm lines in order to study the effects of the incident laser fluence by the presence of overlapped spots on the tensile strength.

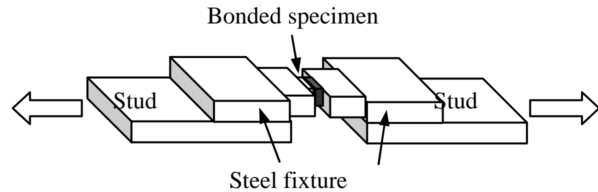


Fig. 5 Microtensile test fixture for TLB specimen

In order to characterize the laser bonding quality, a computer controlled micro tensile tester is used (Fig. 5). The Micro-tester has a 150-N maximum uniaxial load with 1-g load and 100-nm displacement resolutions. The bonded sample is adhered to the steel fixture using epoxy resin, while, the steel fixture is connected to a pull stud. The maximum strength when the substrates begin to peel off is recorded. The bonding strength is calculated by dividing the load needed to separate the bonded by the bonded area.

The bonded interface is analyzed with Auger Electron Spectroscopy (AES) and X-ray Photoelectron Spectroscopy (XPS) in order to determine if drifting or diffusion of atoms occurs at the interface. AES and XPS are the most commonly used techniques for surface analysis with 1 ~ 5 nm below the surface of interest on conducting and semi-conducting solids.

Both techniques rely on the emission of secondary electrons from the specimen after the surface has been excited by either electrons or X-rays. AES allows the incident electron beam to be moved from one specimen surface region to another, determining the surface elemental distribution. XPS has a sufficient level of sensitivity to detect spectrum peak position energy shifts, thereby determining chemical bonding states for the sample surfaces.

## RESULTS AND DISCUSSION

Using a nanosecond pulsed Nd:YAG laser bonding system, Pyrex-to-silicon wafers ($8 \times 8$ mm$^2$) were successfully bonded by continuous line geometry. Fig. 6 displays the optical microscope images of line bonding geometry with 2σ (190 μm) pitch in line with a 11σ (1016μm) pitch between lines. There are 4 bonded lines of 5 mm length in each bonding sample.

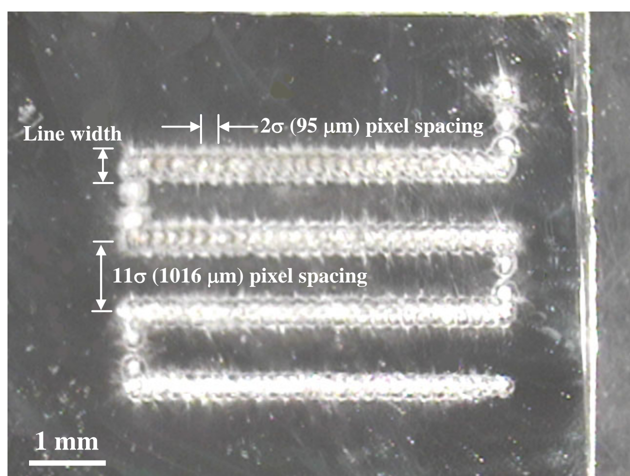


Fig. 6 Optical images of continuous line bonded wafers

Table 2. The width of bonded line

| Line pitch | Line width |
|---|---|
| 95.1μm (1σ) | 332.1 μm |
| 142.7μm (1.5σ) | 320.2 μm |
| 190.2μm (2σ) | 303.6 μm |
| 285.3μm (3σ) | 282.7 μm |

In order to get the bonded area, the bonded line width is measured from the optical images. It is found that the lower line pitch generates a thicker line width, as represented in Table 2. The 1σ (95.1 μm) pitch in line has about 330 μm width, while the 2σ ( 190.2 μm) pitch line has about 300 μm width. The overlapped region is reduced rather than that of 1σ pitch line as shown in Fig. 7. In the 3σ pitch line bonding, the bond spot is barely contacting the subsequent spot, and has about 280 μm diameter. The bonded area is calculated by multiplying the line width by the length.

In continuous line bonding, the bond strengths are measured by a tensile test. For 1σ pitch and 1.5σ pitch lines, the strengths are about 4 MPa with 0.5 ~ 2 MPa of contact pressure. The tensile strengths of 2σ pitch and 3σ pitch lines are about 9 MPa with 1 ~ 2 MPa of contact pressure. In 1σ pitch line bonding, it is observed that the delamination of the bonded sample does not occur at the interface, but rather at the silicon wafer inside. The delaminated silicon surface has a U-shaped channel which is observed during laser micro machining. The surface profile of the delaminated Pyrex glass shows that the removed U-shaped silicon is still attached to Pyrex glass surface. Therefore, it is concluded that high incident laser fluence applied by small pitch may affect the ablation of the silicon wafer. This ablation is responsible for the formation of voids inside of the silicon. The weak bond strength could possible be attributed to the pressure of the voids. It is found that all line bonding strength is dependent a contact pressure, as shown in Figure 8. The bond strength decreases when less than 0.5 MPa contact pressure is applied for 1σ pitch and 1.5σ pitch line bonding. The critical contact pressure for 2σ pitch and 3σ pitch line bonding is generated by 1 MPa.

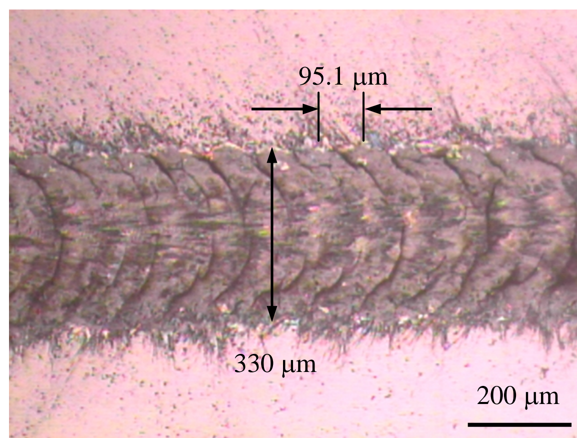


a) 95.1 μm (1σ) pitch line

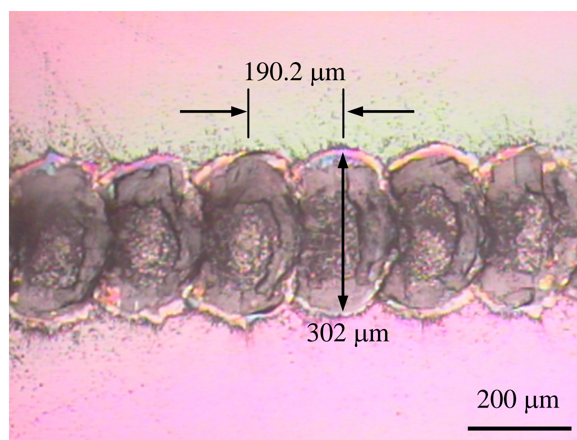


b) 190.2 μm (2σ) pitch line

Fig 7. Optical images of continuous line bonding

In order to determine an optimal laser fluence window, related to bonding geometry, the tensile strengths generated by

different pitches are compared, as shown in Fig. 9. When the line pitch is smaller than 3σ, the bonding geometry represents a continuous line. Single spot bonding provides about 10 MPa of tensile strength, which is comparable to other wafer bonding techniques [6]. In continuous line bonding, a 2σ ~ 3σ pitch is required in order to achieve reliable bond strength. When less than 2σ pitch is provided, the increased incident laser fluence results in a weak bond strength and Pyrex glass damage.

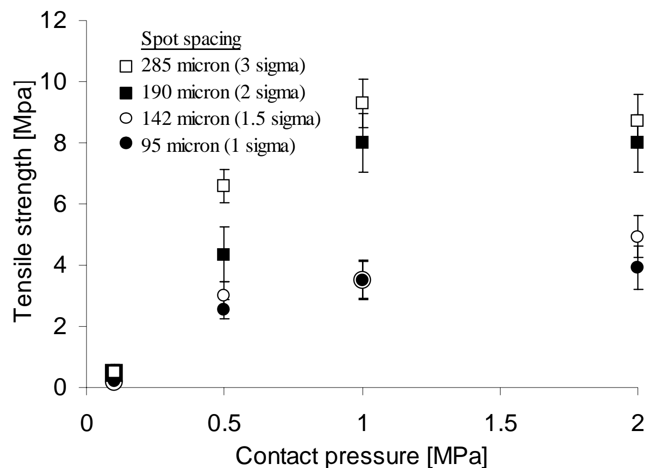


Fig. 8. Contact pressure dependence in line bonding

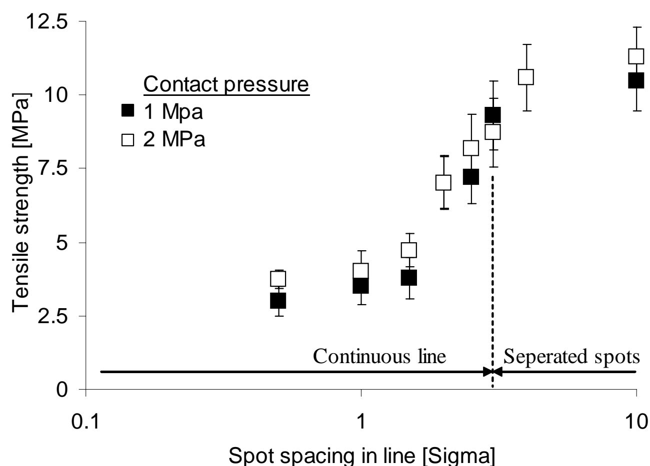


Fig. 9. Oxide thickness dependence on TLB technique

In order to determine if drifting or diffusion of atoms is occurring at the bonded interface, the delaminated bonded interface is analyzed using AES (Physical Electronics, SAM 590) and XPS (Kratos, XSAM800). Since AES uses an electron beam (10 keV) to excite the surface, AES is unable to analyze insulating solids such as Pyrex glass wafers. However, the small spot size (2 μm) of AES provides a good spatial resolution, enabling the user to analyze the laser bonded line with about 300 μm width.

The Auger electron spectra and the distribution profiles at the delaminated silicon surface are represented in depth by Fig. 10.

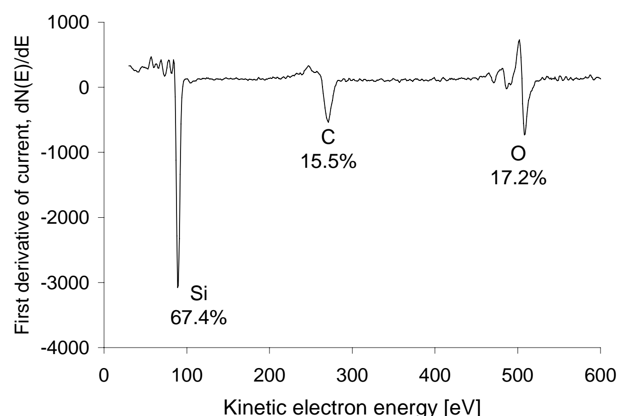


a) AES spectrum at the unbonded surface

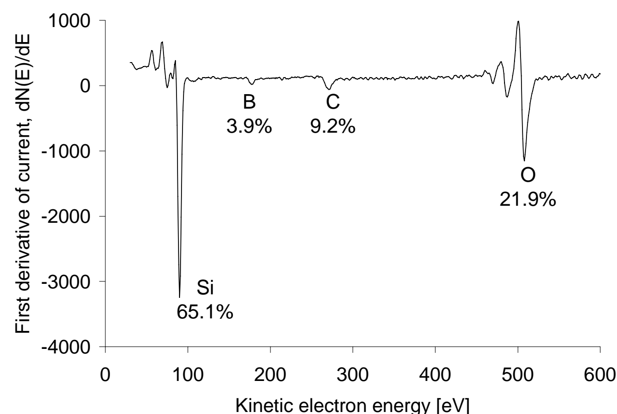


b) AES spectrum at the bonded interface

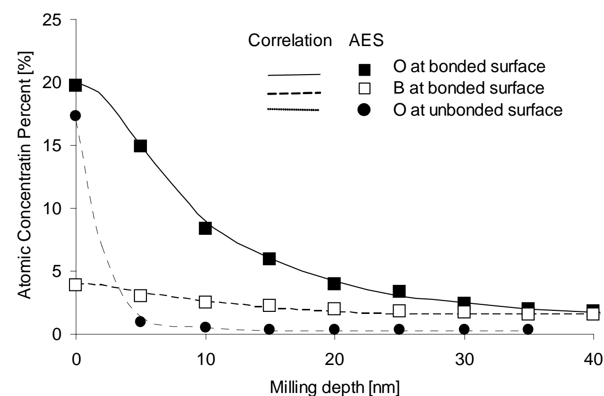


c) The distribution of boron and oxygen at the delaminated silicon surface by Ar ion milling (4 keV)

Fig. 10 AES spectrum and distribution profile in depth at delaminated silicon surface

AES determines if the used silicon wafer surface has a thin native oxide layer and evidence of carbon contamination from air exposure (Fig. 10.a). At the bonded surface, boron (B) is detected, and the atomic concentration percentage (21.9 %) of oxygen (O) on the bonded interface is measured at a slightly larger level than (17.2 %) on the native oxide layer, as shown in Fig. 10.b. Since Pyrex glass wafers consist of 80 % $SiO_2$, 10 % $B_2O_3$, and 5 % $Na_2O$ chemical contents [7] and the used

silicon wafer has no dopants, the boron and the increased oxygen level are diffused from Pyrex glass. Fig. 10.c shows the depth profiles of the boron and the oxygen of bonded interface, milled by a 4-keV Ar ion at a 5-nm/min milling rate. While the thin native oxide layer is removed by 5-nm milling, the boron and the oxygen at the delaminated surface are distributed relatively deep into the silicon substrate. For the sake of comparison, the atomic concentration of O before TLB is also presented in Fig. 10.c. This comparison indicates that the O level reduces to less than 1% after the 5-nm milling. Stated differently, this indication means that the original oxide layer is about 5-nm thick. A strong diffusion process occurs during TLB, this is beneficial since diffused bonds are always desirable in bonding. The reason that strong diffusion exists is that the very thin layers of Si and Pyrex glass which are near the interface (approximately 35-nm thick in the present case) are melted during TLB. The melting generates B and O diffusion. In TLB, the laser beam penetrates the transparent Pyrex glass and is absorbed by the thin surface layer of the opaque Si. The absorbed energy creates a melting zone in the interface which is partially transferred to the surrounding area, melting a thin layer of the contacted Pyrex glass. This interface melting zone can provide a favorable environment for the formation of strong chemical bonds between the transparent Pyrex and opaque Si. The melting zone is thick enough to eliminate the contact resistance and create sufficient intermixing of the two bonded materials in order to form strong chemical bonds.

Since XPS uses X-rays to excite the surface of the material, XPS can analyze conducting and semi-conducting solids as well as insulating solids. Using XPS, both of the delaminated and the bare (after RCA cleaning) Pyrex & silicon surfaces are analyzed. Since the spot size of XPS is 2 ~ 3 mm, Pyrex and silicon wafers ($8 \times 8$ mm$^2$) are bonded with multiple laser bonded spots with 300 μm spot spacing, 300 μm is the focused laser beam size. Figure 11 represents the X-ray photoelectron spectra for the bare and the delaminated wafer surfaces. XPS detects spectrum peak-position energy shifts for the determination of chemical bonding states for the sample surfaces. Using the bare silicon surface as a comparison, XPS measurement indicates that the amount of Si bonded to O (forming $SiO_2$) is higher at the delaminated silicon surface, as shown in Figure 10.a. At the delaminated Pyrex surface, the pure silicon is measured at only a slightly increased level. The bare Pyrex is vacant of pure silicon, as shown in Fig. 11.b. On the bare Pyrex surface, most of the O is incorporated into $SiO_2$. In addition to O in $SiO_2$, the delaminated Pyrex surface has evidence of other O as part of other oxidized substances. These substances drifted from inside the Pyrex, as shown in Fig. 11.c. It is implied that the temperature gradient at the interface, generated by the focused laser energy causes a drift of the oxidized substances ($B_2O_3$ or $Na_2O$) in Pyrex glass to the interface. The oxygen diffusion towards the melted silicon surface therefore results in the formation covalent Si-O bonds between two wafers.

## CONCLUDING REMARKS

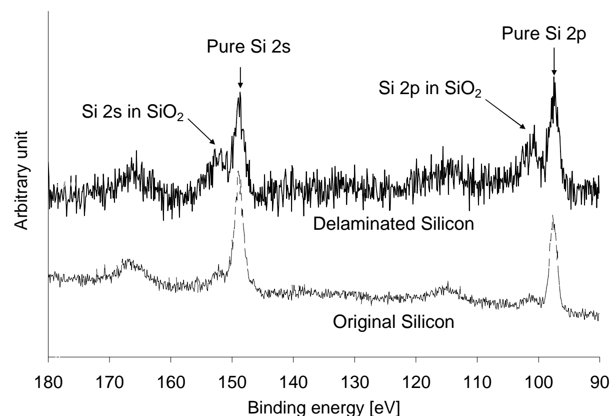


a) XPS spectrum for Si on the silicon surface

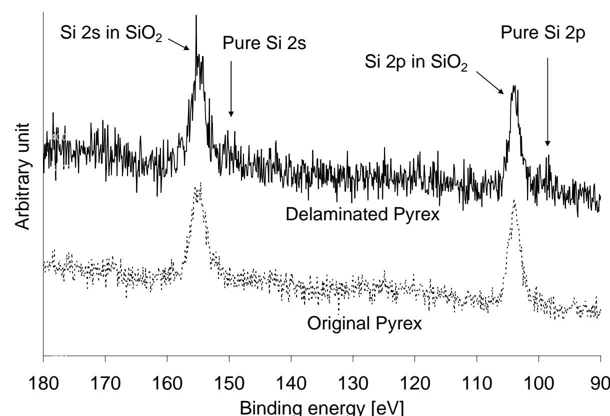


b) XPS spectrum for Si on the Pyrex surface

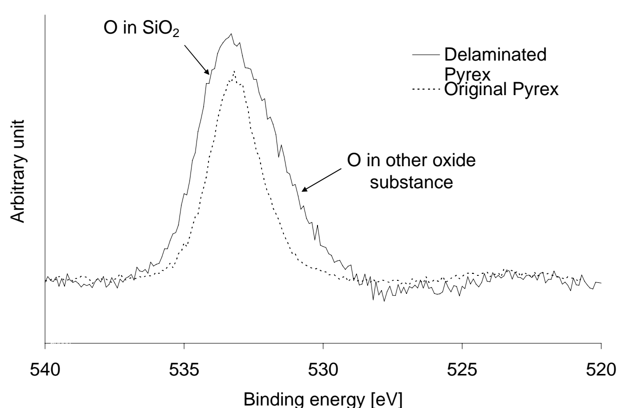


c) XPS spectrum for O on the Pyrex surface

Fig. 11 XPS spectra at the bonded interface and the bare silicon & Pyrex surfaces

In this paper, the continuous line bonding by the TLB technique is implemented and characterized using a nanosecond pulsed Nd:YAG laser. Pyrex and silicon wafers are bonded by continuous lines, and generated with overlapped single bond spots. The influences of contact pressure and laser fluence are examined and evaluated by varying the laser scanning speed and analyzing the bond strength.

In continuous line bonding, 2σ ~ 3σ pitch is required to achieve a reliable bond strength. An application of less than 2σ pitch provides too much incident laser fluence resulting in weak bond strengths and Pyrex glass damage. The critical contact pressure for 2σ pitch and 3σ pitch line bonding is 1 MPa. Using AES and XPS, it is found that the temperature gradient at the interface generates the drift of the oxidized substances in Pyrex glass to the interface. It also proves that the temperature at the interface increases to the melting temperature of silicon by the high intensity laser energy. The oxygen diffusion towards the melted silicon surface results in the formation of covalent Si-O bonds between the two wafers. Tensile tests measuring the bond strength of bonds generated by the TLB technique are comparable with the strengths resulting from conventional wafer bonding techniques.

## ACKNOWLEDGMENTS

The authors gratefully acknowledge the support of this study by the US National Science Foundation under Grant No. DMI-0423457and CMS-0115828. Special thanks are directed to Messrs D. Kingsbury and T. Karcher of Arizona State University for helping with the microtensile test, and with AES & XPS measurements, respectively. Thanks are also due to Misses Elizabeth Marie Nicol and Yariela Mejia, and Messrs Timothy M. Russell and Jeremiah J. Gutierrez-Jensen of Arizona State University for their help in developing the transmission laser bonding technique and preparing this paper.

## REFERENCES

[1] K. Mitani and U. M. Gösele, "Wafer Bonding Technology for Silicon-On-Insulator Applications: A Review" Journal of Electronic Materials vol. 21, no. 7, 1992, pp.669-676

[2] M.B. Cohn, K.F. Bohringer, J.M. Noworolski, A. Singh, C.G. Keller, K. Goldberg, and R. Howe, "Microassembly Technologies for MEMS" Proceedings of the SPIE-The International Society for Optical Engineering, Santa Clara, California, September 1998, vol. 3512, pp.2-16

[3] M.J. Madou, *Fundamentals of Microfabrication: The Science of Miniaturization*, 2nd ed., CRC, Boca Raton, FL, 2002

[4] M.J. Wild, A. Gillner, and R. Poprawe, "Locally Selective Bonding of Silicon and Glass with Laser" Sensors and Actuators A 93, 2001, pp.63-69

[5] R. Witte, H. Herfurth, and S. Heinemann, "Laser Joining of Glass with Silicon", Proc. SPIE-The International Society for Optical Engineering v 4637, San Jose, USA, January 2002, pp.487-495

[6] J-.S. Park and A.A. Tseng, "Development of Transmission Laser Bonding Technique for Wafer-Level MEMS Packaging" International Wafer-Level Packaging Congress (IWLPC), San Jose, California, October 2004

[7] N.P. Bansal and R.H., Doremus, "*Handbook of Glass Properties*", Academic Press, New York, NY, 1986